THE BOW ECHO AND MCV EXPERIMENT

Observations and Opportunities

BY CHRISTOPHER DAVIS, NOLAN ATKINS, DIANA BARTELS, LANCE BOSART, MICHAEL CONIGLIO, GEORGE BRYAN, WILLIAM COTTON, DAVID DOWELL, BRIAN JEWETT, ROBERT JOHNS,* DAVID JORGENSEN, JASON KNIEVEL, KEVIN KNUPP, WEN-CHAU LEE, GREGORY MCFARQUHAR, JAMES MOORE, RON PRZYBYLINSKI, ROBERT RAUBER, BRADLEY SMULL, ROBERT TRAPP, STANLEY TRIER, ROGER WAKIMOTO, MORRIS WEISMAN, AND CONRAD ZIEGLER

The field campaign, involving multiple aircraft and ground-based instruments, documented numerous long-lived mesoscale convective systems, many producing strong surface winds and exhibiting mesoscale rotation.

While the observational study of mesoscale convective systems (MCSs) has been active since the 1940s (e.g., Newton 1950 and references within), until the Bow Echo and Mesoscale Convective Vortex Experiment (BAMEX) there were no studies designed to sample multiscale aspects of these systems throughout the majority of their life cycles. Previous field studies such as the Oklahoma-Kansas Preliminary Regional Experiment for Stormscale Operational and Research Meteorology (STORM)-Central (PRE-STORM) (Cunning 1986) were geographically fixed by the ground-based instrument networks employed. The unique observing strategy of BAMEX relied on the deployment of highly mobile observing systems, both airborne and ground based, supported by the enhanced operational

observing networks [e.g., Weather Surveillance Radar-1988 Doppler (WSR-88D)] over the central United States. Unprecedented high-density kinematic and, especially, thermodynamic observations were obtained within and near MCSs as they evolved.

The field phase of BAMEX was conducted between 20 May and 6 July 2003 and was based at MidAmerica St. Louis Airport (MAA) in Mascoutah, Illinois (near St. Louis, Missouri). During the field phase, life cycles of MCSs occurring over a large portion of the central United States were examined. Two types of systems were emphasized—one producing severe surface winds (bow echoes), and the other producing long-lived mesoscale convective vortices (MCVs) capable of initiating subsequent convection. Although these two phenomena represent useful conceptual archetypes of organized convection, many bow echoes feature pronounced mesoscale rotation. In fact, the broad objective of BAMEX may be summarized as the study of rotationally dominated MCSs.

This article presents an overview of the objectives and experimental design of BAMEX (section 2), followed by a brief summary of selected observations to highlight both the phenomena sampled and the capabilities of different observing platforms (section 3). We conclude with a discussion of some of the lessons learned from operations and the scientific opportunities that lay ahead.

SCIENCE OBJECTIVES AND EXPERIMENTAL DESIGN. *Bow echoes.* Convectively produced windstorms pose a significant hazard to life and property over much of the United States during the spring and summer months. The longer-lived, larger-scale events have been given the generic name of "derecho" (Johns and Hirt 1987). Most derechoes are manifestations of "bow echoes," first described in detail by Fujita (1978; see also Weisman 2001) and most easily identified by their characteristic bow-shaped pattern of high reflectivity on radar images. Key kinematic features of bow echoes include a strong leading-line updraft followed by an intense downdraft and divergent, cold outflow at the surface. The outflow is often accompanied by an intense, rear-inflow jet and a weak-reflectivity region (a "notch") behind the apex of the bow (Burgess and Smull 1993; Przybylinski 1995). Additionally, a dominant cyclonic vortex and weaker anticyclonic vortex are usually evident in the lower to middle troposphere behind the northern and southern ends of the bow, respectively (referred to as "bookend" or "line end" vortices; Weisman 1993). Bow echoes are observed over a range of scales, from tens to a few hundred ki-

lometers in horizontal extent (Klimowski et al. 2000), and can occur as isolated entities or embedded within larger squall lines. Lifetimes vary from tens of minutes to several hours.

The severe, straight-line winds in bow echoes may result from local acceleration of the surface wind within the pressure gradient created by the mesoscale, high pressure region (the "mesohigh") within the surface cold pool. The cold pool, in turn, depends on the structure and strength of the rear-inflow jet (e.g., Smull and Houze 1987) as it entrains drier midlevel air into the mesoscale downdraft, enhancing evaporative effects. The production of negative buoyancy also depends on the microphysical composition of the stratiform precipitation region (where the rear-inflow jet resides). An alternative explanation is that damaging winds result from meso-γ-scale vortices near the surface along the leading edge of the bow echo (Trapp and Weisman 2003). Yet another possible mechanism, purported to explain the intriguing instances of nocturnal wind events, involves internal gravity waves produced from perturbations of the stable boundary layer by deep convection (Bernadet and Cotton 1998). However, the relative magnitudes and importance of these various contributions to surface winds have not yet been quantified.

Few Doppler radar precursors of damaging wind with bow echoes exist to date. Schmocker et al. (1996) found that near the forward (downwind) flank of the convective line, a midaltitude radial convergence (MARC) signature often preceded the bowing of the reflectivity field and subsequent severe straight-line outflow at the surface. Miller and Johns (2000) noticed that extreme damaging winds in derechoes were at times due to high-precipitation (HP) supercells embedded within a convective line. Recent observational studies also suggest the importance of preexisting, line-normal surface boundaries to the formation, propagation, and severe weather associated with bow echoes (e.g., Przybylinski et al. 2000; Schmocker et al. 2000). Such boundaries locally augment horizontal convergence and the horizontal and vertical components of vorticity. This local modification can favor more vigorous convective cells with attendant rotation and stronger surface winds.

In addition to their association with strong, straight-line surface winds, there is also a link between bow echoes and tornadoes (e.g., Fujita 1978; Forbes and Wakimoto 1983; Przybylinski 1995; Pfost and Gerard 1997; Funk et al. 1999). A recent study by Trapp et al. (2004, manuscript submitted to *Wea. Forecasting*) suggests that tornadoes within convective lines account for up to 20% of all tornadic events

nationwide. Also, contrary to popular belief, such tornadoes can be quite strong and long-lived. However, unlike the case of tornadoes spawned from supercell storms, there are no systematic radar signatures preceding tornadoes within convective lines. The incipient rotation usually appears first near the ground just a short time before the tornado forms (e.g., Trapp et al. 1999). The fact that nonsupercell tornadoes develop primarily northward of the apex of the bow (Forbes and Wakimoto 1983) has not yet been explained.

Numerical modeling studies to date have reproduced with some success the observed spectrum of bow-echo phenomena, ranging from strong, bow-shaped lines of cells, forced by a strong surface cold pool and deep lifting along the cold pool's edge, to highly organized systems with strong bookend vortices and elevated rear-inflow jets (e.g., Weisman 1993; Weisman and Davis 1998; Coniglio and Stensrud 2001). Weisman and Trapp (2003) and Trapp and Weisman (2003) have further documented the ability of numerical models to generate intense surface mesovortices, which are perhaps analogous to rotating cells thought to produce damaging winds in some cases. However, sufficient observations have generally been lacking to confirm the dynamics inferred from such simulations.

Mesoscale convective vortices. Composite studies (Maddox 1983; Cotton et al. 1989) have revealed that midtropospheric MCVs of 50–300-km radial extent may be a common structural component of many large MCSs in relatively weakly sheared environments. The mesoscale vertical motion within the stratiform region of MCSs is believed to provide the necessary vortex stretching to induce MCS-scale cyclonic rotation (Bartels and Maddox 1991). Both simulations (Davis and Weisman 1994; Olsson and Cotton 1997) and observations (Bartels and Maddox 1991) have indicated that MCVs are balanced vortices and capable of persisting well beyond the cessation of the strong convection from which they were spawned (Menard and Fritsch 1989; Fritsch et al. 1994; Bartels et al. 1997). These long-lived MCVs have been observed to initiate and focus subsequent heavy rainfall with attendant flooding (Bartels and Maddox 1991; Bosart and Sanders 1981; Fritsch et al. 1994; Trier and Davis 2002). Some MCVs that form or move over warm oceans have been hypothesized to initiate tropical cyclogenesis (Bosart and Sanders 1981; Harr and Elsberry 1996; Bister and Emanuel 1997; Ritchie and Holland 1997; Raymond et al. 1998).

The process of MCV formation has yet to be well observed; hence, collecting observations adequate to understand mechanisms of MCV formation is an important objective of BAMEX. Idealized convection-resolving numerical simulations (e.g., Skamarock et al. 1994; Davis and Weisman 1994; Weisman and Davis 1998; Cram et al. 2002) have shown that systematic tilting of horizontal vorticity associated with MCS-generated buoyancy gradients is responsible for the development of vertical vorticity that is subsequently enhanced by midtropospheric convergence of planetary vorticity. Here the simulated convection resembles the frequently observed asymmetric squall-type MCS (e.g., Houze et al. 1989, 1990; Blanchard 1990; Loehrer and Johnson 1995). While this type of convective organization is common, the few published observations of MCVs spawned from this type of MCS (e.g., Brandes 1990; Jorgensen and Smull 1993; Scott and Rutledge 1995; Knievel and Johnson 2003) have lacked the spatial and temporal data coverage to confirm the basic vorticity generation mechanisms deduced from the simulations. Moreover, both detailed case studies (Bartels et al. 1997) and MCV climatologies (Davis et al. 2002) have indicated that MCVs can, and often do, form within mesoscale areas of convection that are not characterized by this type of convective organization.

A central issue addressed in BAMEX is how new convection is initiated and organized in the vicinity of long-lived MCVs. While it is clear from previous work that MCVs tend to enhance convection downshear and suppress convection upshear of their center (e.g., Raymond and Jiang 1990; Trier et al. 2000), it is not clear to what extent the mechanism of balanced lifting acts independently from planetary boundary layer evolution to initiate convection. For instance, afternoon convection in the vicinity of MCVs has been observed to form along convective outflow boundaries and at the edge of the MCV cloud shield, where thermally direct solenoidal circulations are likely to occur (Trier et al. 2000).

The longevity of MCVs is strongly influenced by whether new convection initiates within their circulation (Fritsch et al. 1994; Trier et al. 2000; Davis et al. 2002). The mechanism by which new convection intensifies the MCV and causes its circulation to penetrate into the planetary boundary layer have been discussed by Rogers and Fritsch (2001) and Davis and Trier (2002) based on different case studies, but a more general perspective of the interaction between MCVs and convection is lacking. It is possible that recent theoretical analysis of the tropical cyclogenesis problem (e.g., Montgomery and Enagonio 1998)

can augment our understanding of convection effects on midlatitude MCVs. It is also possible that better observations of MCVs and their attendant convection will enhance our understanding of tropical cyclogenesis.

Design of BAMEX operations. FACILITIES AND THEIR DEPLOYMENT. Facility deployment during the field phase of BAMEX was based on a system-following strategy, adopted to observe the life cycle of MCSs. Such a strategy was possible owing to the nearly contiguous WSR-88D coverage over the central United States and the relatively dense network of operational soundings, wind profilers, and surface observations. Thus, the highly mobile platforms could roam over these surface facilities without being tied to a special instrumented domain, unlike in earlier mesoscale convection field projects. The objectives of BAMEX required documenting structures on many scales: meso-γ scale (intense convective cells, outflow boundaries), meso-β scale (rear-inflow jets, vortices), and meso-α scale (large MCVs, environmental structure). The mobile facilities used during BAMEX (Table 1) consisted of P-3 aircraft from the Naval Research Laboratory (NRL; Fig. 1a) and from the National Oceanic and Atmospheric Administration

(NOAA; Fig. 1b), each equipped with fore- and aft-scanning X-band Doppler radars mounted in the tail, a Learjet (Fig. 1c) leased from Weather Modification, Inc. (WMI), equipped with dropsondes deployed from roughly 12 km AGL, and an array of mobile ground-based observing systems (Figs. 1d,e).

It was convenient to distinguish observational strategies for mature MCSs (whether a bow echo or not) from those for remnant MCVs, the latter associated with diminishing or scattered precipitation. In Fig. 2 we depict ideal system-relative aircraft flight tracks and ground-based facility deployment for these two scenarios. For MCS missions (Fig. 2a), the objec-
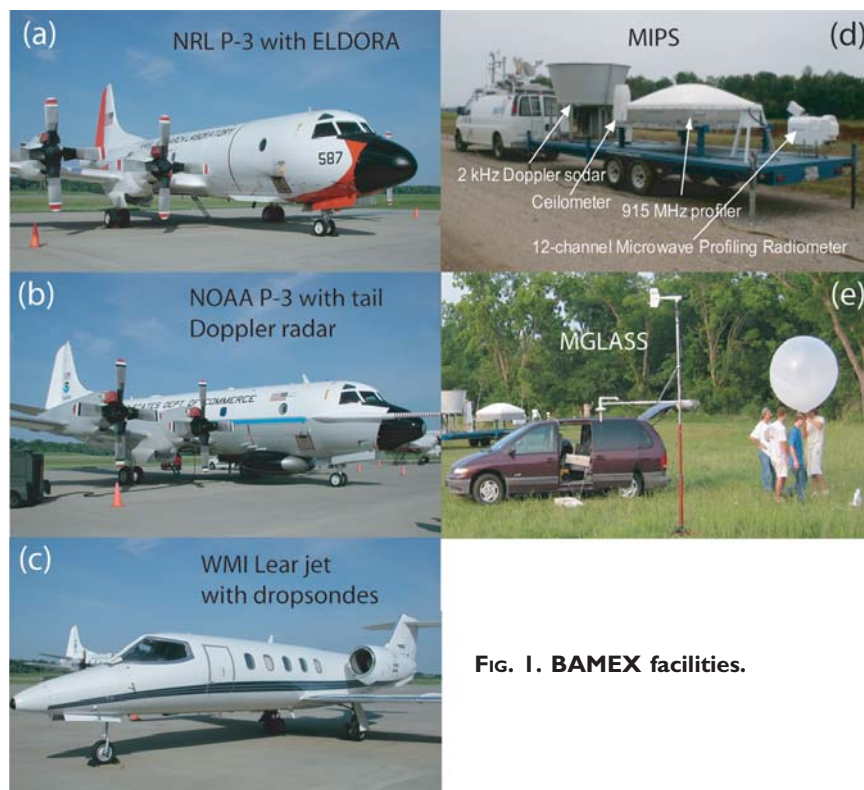

FIG. 1. BAMEX facilities.

TABLE 1. BAMEX facilities, principal investigators (PI), and usage during the project.

FACILITY	PI	Usage
NOAA P-3 Aircraft	D. P. Jorgensen (NSSL)	128 h
Microphysical measurements on NOAA P-3	G. McFarquhar, R. Rauber, B. Jewett (UIUC)	
NRL P-3 Aircraft (ELDORA)	R. Wakimoto (UCLA), W.-C. Lee (NCAR)	114 h
High-level jet	C. A. Davis (NCAR)	102 h/464 sondes
MIPS	K. Knupp (UAH)	
MGLASS (2)	M. Weisman (NCAR)	260
Mobile probe	D. Dowell (NCAR)	

tive of the aircraft, collectively, was to retrieve wind, temperature, humidity, and microphysical data within MCSs and sample the mesoscale structure of their environment. The ground-based observing system (GBOS) was focused on obtaining measurements of state parameters in the boundary layer and lower troposphere within and ahead of approaching MCSs (Fig. 2a). For mature MCVs, the P-3s were not deployed unless there was an extensive precipitation area accompanying the MCV because the Doppler radars did not have the sensitivity for clear-air mapping out to their maximum ranges. The objective of the GBOS was to augment dropsondes and assist in characterizing the destabilization of the boundary layer in the presence of an MCV.

The rapid scanning capability of the Electra Doppler radar (ELDORA) on the NRL P-3 made it ideal to scan the convective region of MCSs, mapping the kinematic structure of the leading convective line and the rear-inflow current immediately behind the line (to the extent allowed because of attenuation). The

NRL P-3 remained ahead of the line (i.e., generally to the east of an eastward-moving line) and flew legs roughly 50–100 km in length at an altitude around 1.5 km MSL.

The primary responsibility of the NOAA P-3 (*N-42*) was to map the region to the rear (i.e., to the west) of the convective line. The typical altitude range for this aircraft was 10,000–14,000 ft (3–4 km) MSL. Spiral ascent/descent patterns were occasionally flown to collect vertical profiles of microphysical data in the well-developed stratiform rain region. These data were from the two-dimensional cloud (2D-C) and two-dimensional precipitation (2D-P) Particle Measuring System (PMS) laser spectometer probes (cloud and particle imagers, respectively), mounted under the wing of the P-3. These data are important for evaluating the microphysical contribution to the downdrafts within MCSs. In about half of the BAMEX intensive observing periods (IOPs) the legs of the NRL P-3 were synchronized with the legs of the NOAA P-3 for collecting "quad Doppler" data or simultaneous observations of common points (Jorgensen et al. 1996), which enables the derivation of substantially more accurate vertical velocities in the convective region. Both ELDORA and the NOAA P-3 Doppler radars used staggered pulse-repetition-frequency techniques to extend their unambiguous Nyquist velocities to beyond 50 m s^{-1} to avoid radial velocity folding problems (Jorgensen et al. 2000).

The WMI Learjet typically flew at nearly 40,000 ft (12 km) MSL for 3–4 h. Dropsondes from the jet sampled the environment of MCSs and the stratiform region containing vortices and the rear-inflow current. Closely spaced (< 100 km) soundings offer a critical set of data often missing from field studies of convection. Beside providing information about mesoscale structures within and outside MCSs, these data are important for radar-based thermodynamic retrievals and research in experimental data assimilation.

The GBOS consisted of the Mobile Integrated Profiling System (MIPS) from the University of Alabama at Huntsville as well as three Mobile GPS/Loran Atmospheric
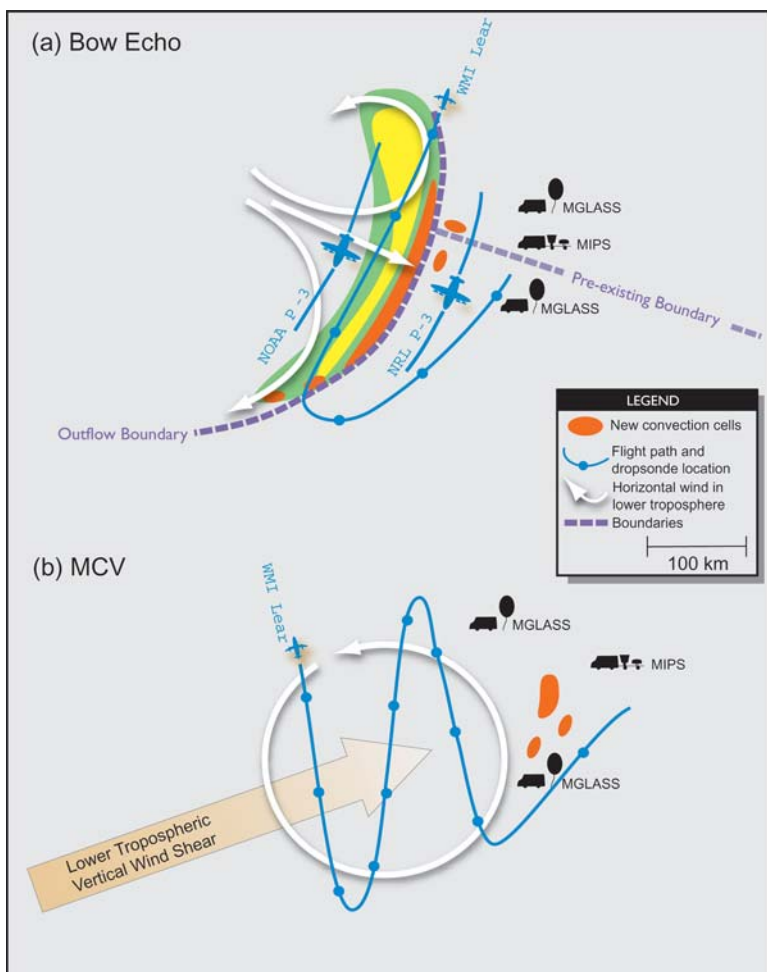

FIG. 2. Schematic of BAMEX facility deployment.

Sounding System (MGLASS) units from the National Center for Atmospheric Research (NCAR) and a mobile probe vehicle. The MIPS comprises a Doppler sodar, 915-MHz wind profiler, radiometer, ceilometer, electric field mill, and a disdrometer. One of the MGLASS units also resided with the MIPS. Typically the GBOS was deployed along a line parallel to an approaching MCS with MIPS in the middle. MGLASS units were located on either side of any boundaries that existed ahead of the MCS.

An additional component of the BAMEX observing strategy was detailed damage surveys performed within 1–2 days following the occurrence of a bow echo. These surveys were conducted both from the ground and from the air, the latter using a small, leased aircraft. The decision to conduct a survey was based on both reports of wind damage and in response to radar signatures of severe weather.

For MCV missions without appreciable precipitation near the vortex, the main deployment was the GBOS and the Learjet with dropsondes (Fig. 2b). The Learjet executed flight legs 200–300 km long across the vortex circulation. GBOS was deployed in a triangle on the downshear side so that the soundings from the triangles could be used to compute a time series of vertical motion. The number of soundings obtained during MCV missions ranged from about 15 to 40, spanning a 3–6-h period.

DOMAIN OF OPERATION. BAMEX was focused in the Midwest, owing to the climatological frequency of bow echoes (Johns and Hirt 1987; Evans and Doswell 2001) and MCVs (Bartels and Maddox 1991; Trier et al. 2000), combined with the concentration of wind profilers, surface mesonetworks, and WSR-88D radars. Shown in Fig. 3 is the geographical extent of BAMEX operations as represented by the location of dropsondes deployed by the Learjet. The aircraft and operations center base was MAA in Mascoutah, Illinois, about 25 miles east of St. Louis. This facility was a civilian airport without substantial commercial air traffic at the time of the project. The location was central to numerous National Weather Service (NWS) forecast offices, especially the St. Louis office, and in the heart of activity of convective systems of interest. All aircraft operations took place at MAA, except for two IOPs where the aircraft had to land elsewhere because of inclement weather near St. Louis. The range of aircraft deployment was roughly 600 km from this location, with a slight bias for westward deployment to sample approaching MCSs. The GBOS was not based at MidAmerica St. Louis Airport. It was forward deployed throughout the project, being re-positioned on a daily basis based on the forecasted location of weather of interest.

COORDINATION OF OPERATIONS. An extraordinary level of operations coordination was required to support simultaneous measurements from three research aircraft and ground facilities in and near developing and strong convective storms that often propagated with velocities in excess of 25 m s^{-1}. The communications network to support BAMEX consisted of cell phones, high-bandwidth data lines, and satellite voice and data links. The project facilities and scientists implemented a network to minimize single points of failure while providing all participants with necessary communications required to conduct a well-coordinated, complex measurement strategy.

BAMEX represented the first extensive use of satellite Internet capability to coordinate multiple aircraft flight patterns in rapidly evolving weather systems. Extensive use was made of ground-based WSR-88D composites, constructed at MidAmerica St. Louis Airport, to adjust (in real time) the flight tracks of the aircraft to maximize the Doppler radar and dropsonde coverage and to ensure that the dropsondes were not deployed above the turboprop aircraft. One innovative aspect of the communications strategy was the use of an Internet "chat room" to keep all principal BAMEX components informed of the rapidly changing weather and observing strategies. Operations coordinators at MAA, aircraft chief scientists on the turboprop aircraft, dropsonde operations on the Learjet, as well as many interested public "lurkers" could monitor the progress of the IOPs and contribute suggestions.

The combined efforts of several groups resulted in a successful field operations coordination. NWS office forecasters and project scientists provided expert forecasting support (see "Forecasting" below). The Atmospheric Technology Division (ATD) of NCAR provided real-time-integrated weather products, and radar and aircraft position information. In addition, the University Corporation for Atmospheric Research (UCAR) Joint Office for Science Support (JOSS) provided the BAMEX Field Catalog and operations support services.

The majority of IOPs required operations at night. On many occasions, operations did not end until 0300–0600 a.m. Perhaps more difficult were the changes from nighttime to daytime operations and back again. These changes were most commonly performed for dropsonde missions so that both the mature, mainly nocturnal MCSs and their remnant MCVs (often evident during the following morning)

could be sampled. To accomplish this, two dropsonde crews were employed as well as a second set of personnel in the operations center.

Coordination of the ground teams with aircraft operations was remarkably successful, occurring in more than half of the IOPs. Ground crews had to cope with nightly changes in lodging, long drives (sometimes exceeding 500 km) on most days, setup in adverse conditions, and redeployment in many instances to respond to changing weather conditions.

FORECASTING. Forecasting was crucial for successful BAMEX planning and operations. In order to entrain as much experience as possible, forecasters from Central Region NWS offices and from the Storm Prediction Center teamed with researchers from NCAR and universities to doubly staff a forecaster (6–48-h forecasts) and two nowcaster (0–6-h forecasts) positions each day. A total of 16 NWS operational personnel and 7 research personnel participated in the forecasting. The heavy emphasis on forecasting was necessitated because of the multiple critical decisions required each day, including where and when to deploy the GBOS, determination of aircraft takeoff times 24-h in advance, and prediction of probable down days (required at least every 7 days).

Three forecast models, each using fully explicit treatments of convection on grid increments of 4 km or less, were run in support of BAMEX. The Regional Atmospheric Modeling System (RAMS; Pielke et al. 1992), the fifth-generation Pennsylvania State University (PSU)–NCAR Mesoscale Model (MM5; Grell et al. 1994), and the recently developed masscoordinate version of the Weather Research and Forecasting (WRF) model (Michalakes et al. 2001) were all integrated daily in near–real time. In a follow-on study, Done et al. (2004, manuscript submitted to *Atmos. Sci. Lett.*) concluded that forecasts of 12–36 h from the WRF model were able to explicitly and realistically represent the mode of convection on the majority of days, and that this information was highly useful in planning aircraft-observing strategies.
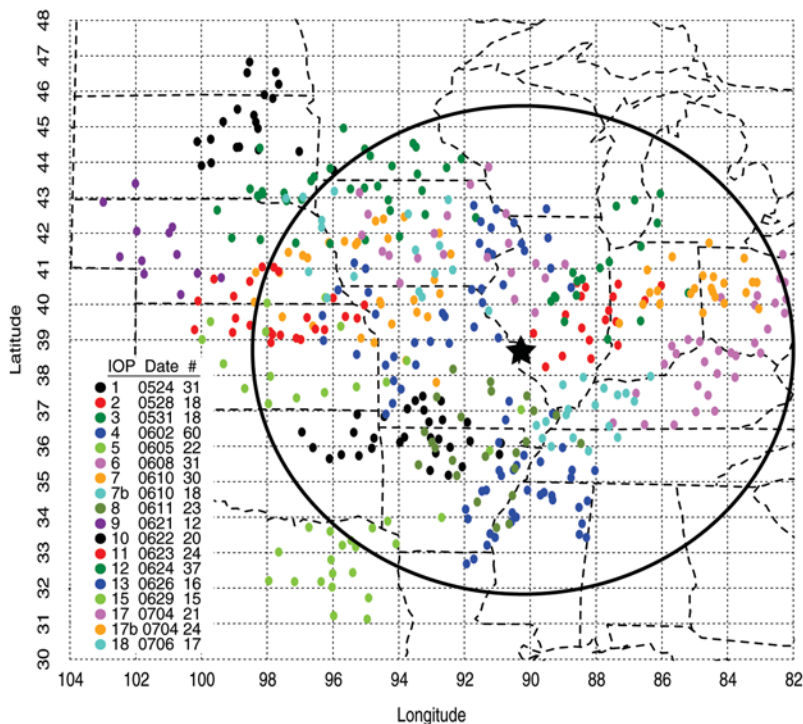

FIG. 3. Locations of dropsondes during BAMEX, color coded by IOP. Black star indicates location of MidAmerica St. Louis Airport. Black ellipse represents 600-km-range ring around MidAmerica St. Louis Airport. The number of dropsondes is lower than that reported in Table 1 because not all dropsondes reported position.

BAMEX IOPS. *Overview.* During BAMEX there were 18 IOP and two non-IOP missions investigating a total of 26 distinct convective systems. Table 2 summarizes the emphases of each case; note that many IOPs have more than one phenomenological focus. A total of 11 bow echoes were observed, with 9 sampled by aircraft. Four of these were particularly severe as judged by radar signatures and damage reports. From the standpoint of facility availability, bow echoes in IOPs 4, 7, and 13 were the best sampled, although IOPs 10, 12, 16, 17, and 18 appear to be excellent datasets as well.

Five mature MCVs were sampled. These were mesoscale vortices that persisted at least several hours beyond the decay of the MCS in which they developed. Although Table 2 lists five developing MCVs as well, the actual number is likely to grow as analysis of Doppler radar data advances. In some instances, MCVs formed within bow echoes. Often, one of the Doppler-equipped aircraft completed a large-scale "survey" pattern following the coordinated multiple aircraft patterns to document any MCV development.

IOP	Location	Nonbowed MCS	Mature MCV	Forming MCV	Bow echo
1: 24–25 May	OK, AR		X[(2, 3, 4)]		X[(5)]
2: 28–29 May	IL, IN	X[(1, 2, 3, 4)]		X[(3, 4)]	X[(2, 3, 4, 5)]
3: 30–31 May	IL, IN	X[(1, 2, 3, 4, 5)]			
4: 2–3 Jun	KS, AR, MS		X[(4)]		X[(1, 2, 3, 4)]
5: 5–6 Jun	TX, AR		X[(1, 3, 4)]		
6: 8 Jun	IN, OH	X[(2, 3, 4)]			
7: 9–10 Jun	NE, IA, MO, KY, TN	X[(4)]		X[(3, 4)]	X[(1, 2, 3, 4, 5)]
8: 11 Jun	AR		X[(4)]		
9: 20–21 Jun	NE	X[(2, 3, 4)]			
10: 22 Jun	SD				X[(1, 2, 3, 4)]
11: 23 Jun	NE, KS	X[(1, 2, 3, 4)]			
12: 24 Jun	NE, IA				X[(1, 2, 4, 5)]
13: 25–26 Jun	IL			X[(3, 4)]	X[(1, 2, 3, 4)]
14: 29 Jun	KS	X[(1, 2, 3)]			
15: 29–30 Jun	KS		X[(1, 3, 4)]		
16: 2-3 Jul	MN				X[(1, 2, 3)]
17: 4–5 Jul	IA, IL, IN	X[(1, 4)]		X[(3, 4)]	X[(3, 4, 5)]
18: 5–6 Jul	NE, IA	X[(1, 2, 3, 4)]		X[(3)]	X[(2, 3, 4, 5)]
Other missions					
7–8 Jun	TX	X[(1)]			
10 Jun	MO, IL				X[(5)]

Many more MCVs occurred during BAMEX than were observed during IOPs. A rough estimate from satellite and radar data suggests 35–40 mesoscale vortices formed within MCSs during BAMEX. An exceptional period was 11–12 June when six MCVs were detected.

Bow echoes. Here, we briefly summarize two bow echoes, IOPs 7 and 12, occurring on 9–10 June and 23–24 June, respectively. In Fig. 4 are shown the tracks of these bow echoes. The isochrones were constructed by drawing a line approximating the location of the center of the leading convective line based on Weather Services International (WSI) composite reflectivity Z (maximum in the column) where $Z > 45$ dBZ. Isolated cells are not represented in the figure.

The MCS during IOP 7 formed over northeast Nebraska around 0000 UTC 10 June (Fig. 4). It evinced a double-bow structure early in its evolution (e.g., 0300 UTC; Fig. 4), consolidating later to a continuous line, though still retaining bowed segments (0600 UTC; Fig. 5a). According to severe storm reports archived by the Storm Prediction Center, and confirmed by extensive damage surveys conducted by BAMEX personnel, a concentrated area of wind damage occurred near Emerson, Nebraska (near Sioux City, Iowa), with the small bow-echo segment to the northeast around 0130 UTC. Additional damage occurred in and around Shelby, Nebraska (southeastern Nebraska), with the southwestern-bowed segment between 0100 and 0400 UTC. Typical maximum estimated surface winds were 30–35 m s^{-1}. Damage oc-

curred principally to trees, pivot irrigation systems, and grain silos.

The quad-Doppler retrieval shown in Fig. 5b was constructed from observations made just before 0600 UTC. It shows extensive system-relative rear inflow exceeding 20 m s⁻¹ at 4 km MSL. At this time, surface observations and a subsequent survey indicated no damaging winds. In Fig. 6, we show a cross section through the line based on these same quad-Doppler data. A narrow (~10 km wide) leading convective line is evident, with a maximum reflectivity exceeding 56 dBZ. The leading updraft appears erect, or even tilted slightly downshear, with no evidence of front-to-rear flow in the upper anvil. An elevated rear-inflow jet appears between 2.5 and 5 km AGL. There is evidence of strong subsidence within the jet, and an apparent downward slope toward the front of the line, but the jet does not penetrate below about 2 km AGL, consistent with a lack of damaging surface winds. The maximum jet speed, relative to the leading line, is about 25 m s⁻¹. Given the assumed storm motion of 17 m s⁻¹ toward the southeast (128°), the maximum ground-relative wind was about 42 m s⁻¹. This agrees closely with flight-level data from the NOAA P-3 collected at 3 km AGL. The obvious unanswered question in this case is why the surface winds were not stronger around 0600 UTC, or, alternatively, why the strong rear-inflow jet remained elevated.

Also of note is the apparent lack of a dominant cyclonic line-end vortex on the northeastern end of the bow in the Doppler analysis of Fig. 5b. An anticyclonic vortex is indicated behind the southwest end of the convective line. The lack of a dominant cyclonic vortex contrasts with the evolution of an isolated bow presented by Fujita (1978). Perhaps, given the close proximity of the bowed segments, there was not a sufficiently well-defined break in the convection to allow line-end vorticity generation effects to occur. Such behavior has been noted in quasi-idealized simulations of bowed convective systems (Weisman and Davis 1998).

The bow echo of IOP 12 formed in a similar location and at a similar time of the evening as did IOP 7, but because the former was embedded within gener-
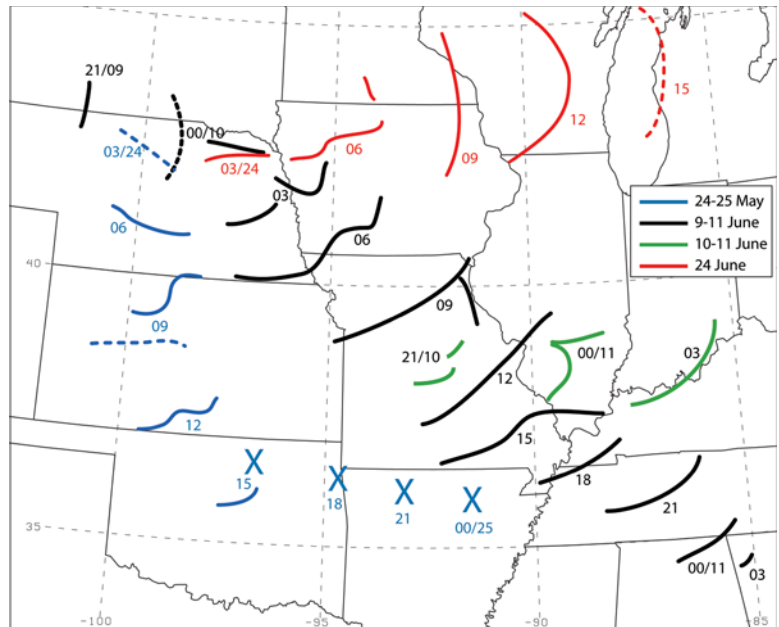

Fig. 4. Isochrones of solid convective lines with maximum reflectivity > 45 dBZ (solid), broken or dissipating lines (dashed), and MCV positions (Xs) for three IOPs. Blue denotes IOP 1 (24 May 2003), black denotes IOP 7 (9–10 Jun 2003), red-orange denotes IOP 12 (24 Jun 2003), and green denotes 10–11 June St. Louis bow echo. Times are UTC in 3-h intervals. The convention HH/DD is used to indicate selected dates.

ally southwesterly flow, it tracked eastward rather than southeastward (Fig. 4). This event featured coordination of the NRL P-3, Learjet, and GBOS. The NOAA P-3 experienced a fuel leak and was forced to abort its mission. Exceptionally good data from ELDORA were obtained as the NRL P-3 traversed the area ahead of a bowed segment in the line (Fig. 7). A maximum outflow exceeding 35 m s⁻¹ was observed around 0630 UTC 24 June.

A sharp gradient in radial wind (within the box in Fig. 7a) suggests an area of large relative vorticity, indicated by a preliminary dual-Doppler analysis as exceeding 1.5 x 10⁻² s⁻¹ (red ellipse in Fig. 7b). Although there was no sighted tornado near this location, and none suggested by a subsequent damage survey of the area, this relative vorticity is of the same order as that in a mesocyclone. Stretching of such vorticity along the outflow boundary, essentially the configuration shown in Fig. 7b, has been hypothesized to lead to some short-lived tornadoes within quasi-linear MCSs (e.g., Fujita 1978).

According to archived Storm Reports, a maximum surface wind of roughly 30 m s⁻¹ was estimated about 30 min prior to this time in conjunction with the bowed segment. Surveyed damage was confined to the area near Washta, Iowa. A time series of wind, tem-
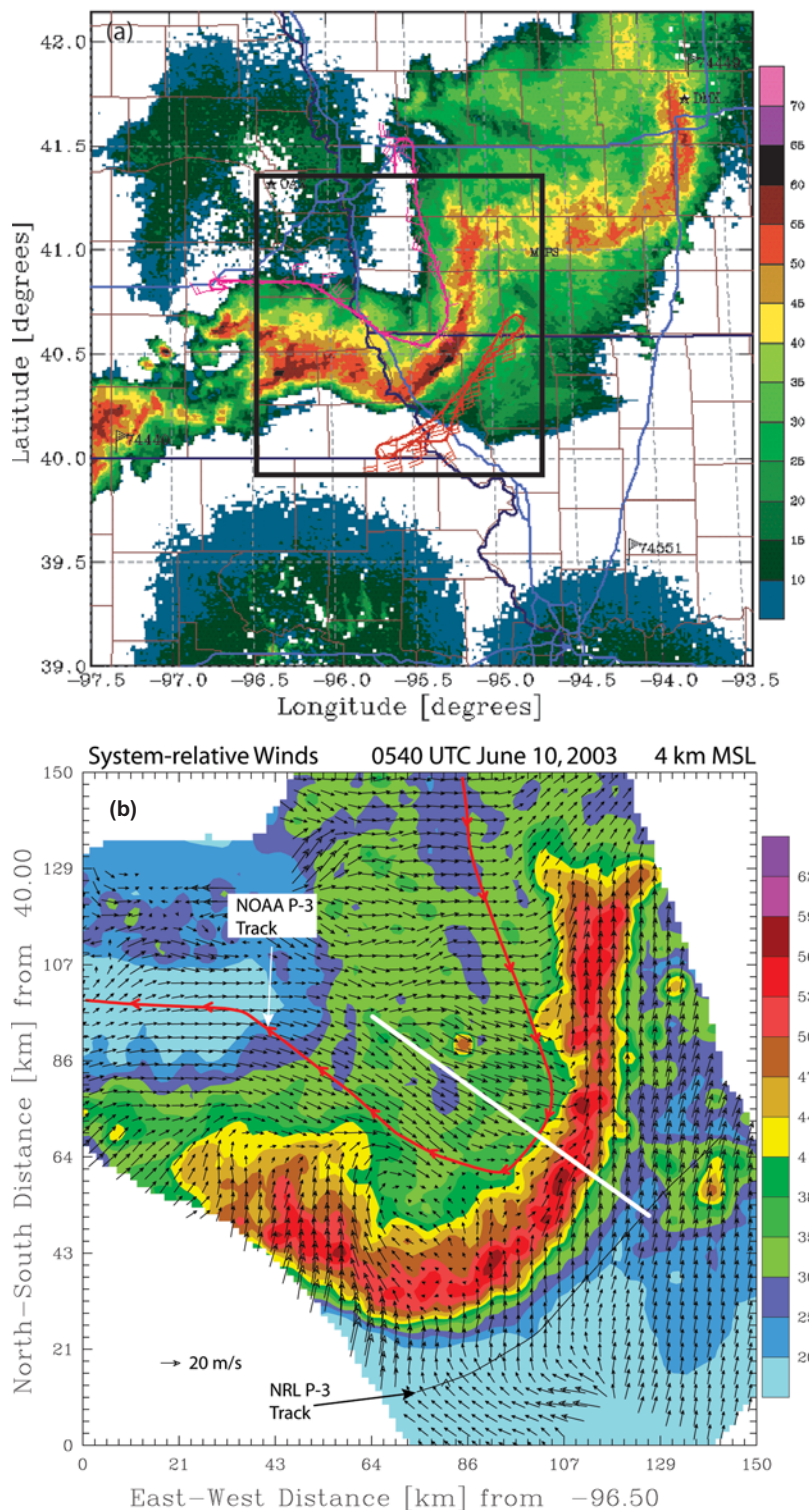
FIG. 5. (a) Base-scan reflectivity composite from WSR-88Ds from 0540 UTC on 10 Jun 2003. NOAA P-3 track is indicated in magenta, NRL P-3 track is shown in red. Box with black outline indicates quad-Doppler analysis domain (Fig. 5b); (b) quad-Doppler retrieval of system-relative winds within a bow echo on 10 Jun 2003. The NRL P-3 flew ahead of the convective line, the NOAA P-3 behind. The line was moving southeastward at about 20 m s⁻¹. White line denotes the location of the cross section shown in Fig. 6.

perature, and pressure from the Iowa Mesonet station at Le Mars (50 km northwest of Washta, 150 km west-northwest of the MIPS position in Fig. 7a) reveals the rapid onset of strong winds following the passage of the out-flow boundary (Fig. 8). The wind direction backed from southeasterly to northeasterly just prior to 0400 UTC, then shifted to west-northwesterly behind the boundary (not shown). The temperature rose slightly after passage of the boundary, then fell steadily by 6°C in the ensuing 12 min. The end of the pressure rise following the boundary passage roughly coincided with the peak wind speed.

The MIPS and MGLASS units were well placed for this event (Fig. 7a). The MIPS observed the gust front passage at about 0640 UTC (Fig. 9a). The strong, shallow updraft at the leading edge was apparent, as was a much deeper updraft of about 15 m s⁻¹ a few minutes later (assuming a terminal velocity v_T of 5 m s⁻¹). The MGLASS-1 unit launched a sounding at 0450 UTC (Fig. 9b). This revealed a low-level (900 hPa) southwesterly jet of 25 m s⁻¹, yielding extremely large vertical wind shear over the lowest kilometer. Vertical shear over the lower and middle troposphere was weak, but strengthened again above 500 hPa. The sounding apparently penetrated the anvil cloud at about 460 hPa (6.5 km MSL), within which the profile was moist adiabatic and approximately saturated with respect to ice. Judging from the inversion at the base of the anvil, the temperature within the cloud was as much as 5°C warmer than within the environment. The buoyancy in the middle troposphere for hypothetically lifted parcels maximized at about 12°C about 500 m below the anvil, even for air parcels lifted

from as high as 2 km MSL. This explains how the MCS could retain its intensity overnight in the presence of a stabilizing boundary layer. However, based on direct observations from the MIPS and a lack of further severe wind reports, it appears that the damaging surface winds ceased following the pronounced outflow event shown in Fig. 7 and did not resume despite the fact that the MCS maintained intensity through 1200 UTC.

Between about 0700 and 0900 UTC, the MCS underwent a dramatic reorganization, becoming a longer (~300 km) convective arc oriented nearly north–south (Fig. 4). The system persisted in this configuration and propagated rapidly eastward at roughly 20 m s^{-1}. As it reached Lake Michigan, the MCS rapidly dissipated around 1400–1500 UTC.

The St. Louis bow echo of 10 June. Around 2000 UTC on 10 June 2003, a small cluster of intense convective

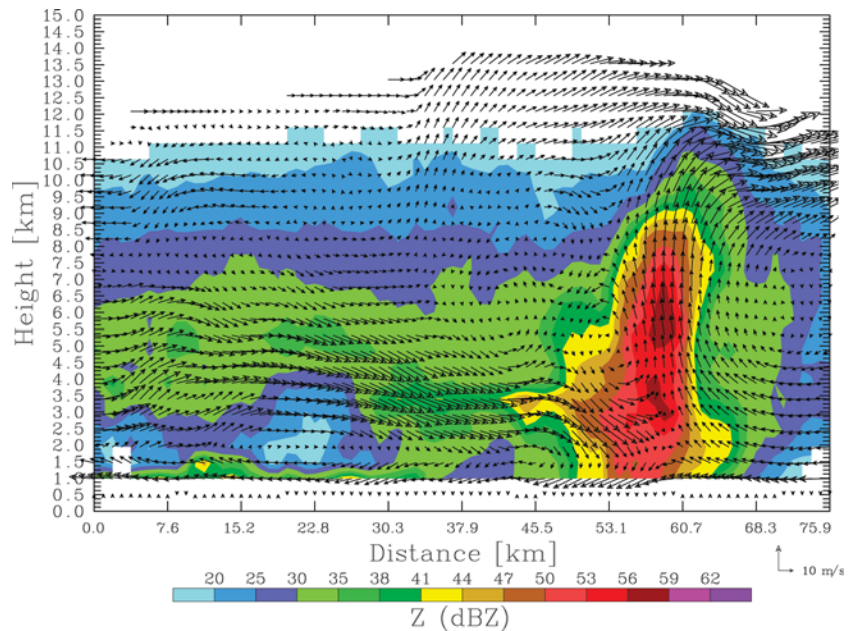cells formed in central Missouri. By 2100 UTC, the area had formed a short, severe convective line

FIG. 6. Cross section from 10 Jun bow echo (see Fig. 5b) produced from quad-Doppler analysis. Shown are system-relative winds and reflectivity (dBZ) in the vertical plane.

FIG. 7. (a) Radial velocity from horizontal scan from ELDORA (altitude approximately 1 km) with flight track shown by dashed line; (b) reflectivity within box shown in panel (a). Red oval indicates vorticity greater than 1.5 x 10^{-2} s^{-1} estimated from preliminary dual-Doppler retrieval.
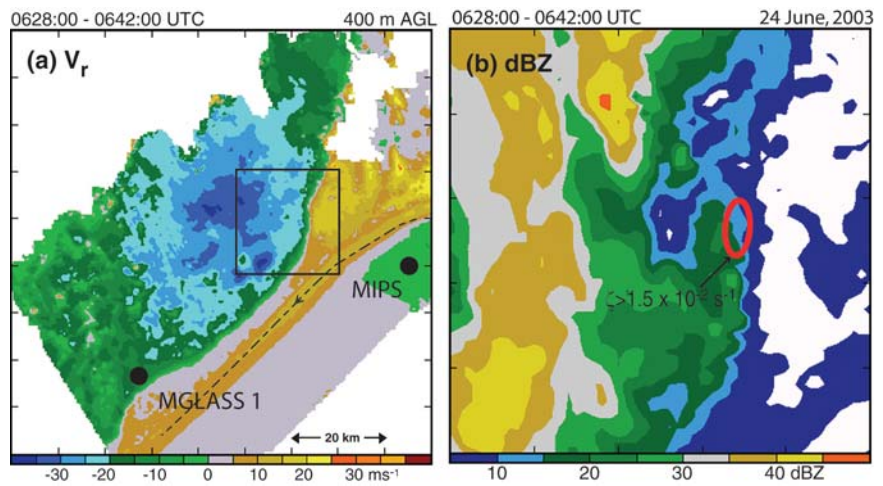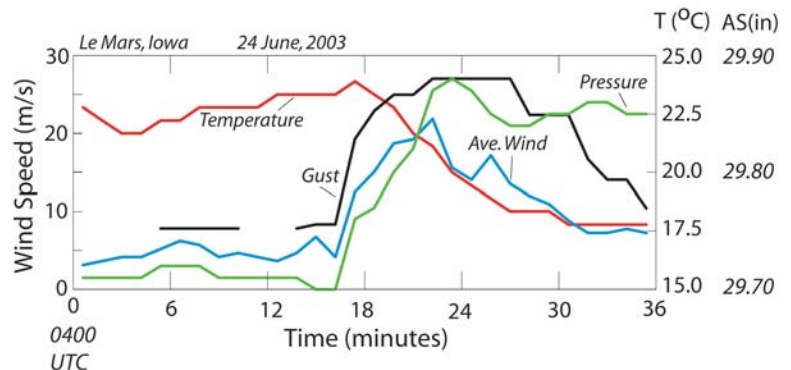

FIG. 8. Time series of 1-min data from Le Mars, IA, Automated Weather Observing Station (AWOS) during a 36-min period following 0400 UTC 24 Jun 2003. Temperature (°C) is in red, wind speed (2-min average) is in blue, wind gust (maximum 5-s average during the previous 5 min), is in black, and altimeter setting [AS; inches of mercury (Hg)] is in green. Note that 0.1" Hg is roughly 3.4 hPa.
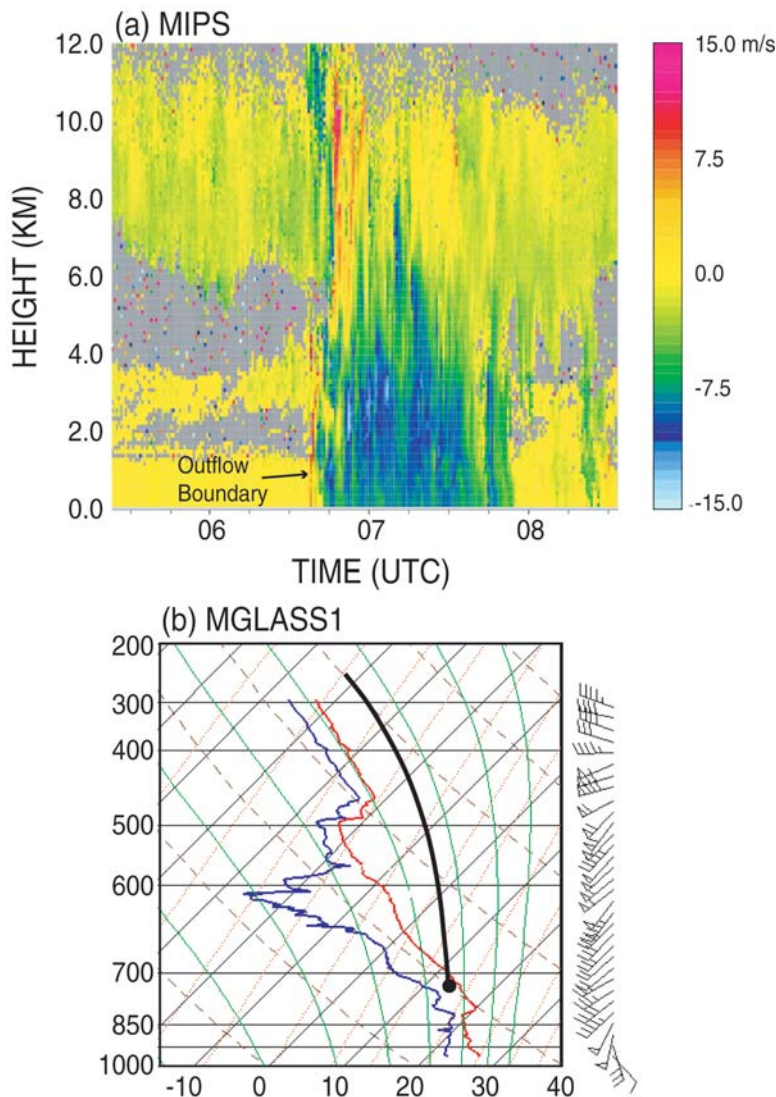
FIG. 9. (a) Time–height cross section of total vertical velocity ($w + v_T$) from MIPS on 24 Jun; (b) MGLASS-1 sounding launched at 0450 UTC 24 Jun. A hypothetically lifted parcel from the top of the inversion near 800 hPa is shown by the heavy solid line, with the black dot denoting the lifting condensation level. See Fig. 7 for location of ground-based instruments.

field), revealed the transit of a wind maximum of 45 m s⁻¹ near 200 hPa just prior to convective initiation, and another westerly jet of about 25 m s⁻¹ near 500 hPa at about the same time (not shown). Thus, the MCS moved about 10 m s⁻¹ faster than any nearby observed wind below about 250 hPa. The convective available potential energy (CAPE), estimated from the Springfield sounding, was in excess of 2700 J kg⁻¹, but CAPE as high as 4000 J kg⁻¹ was estimated in the area of convection initiation. Reports of damaging wind began at 2120 UTC, but increased substantially in frequency and severity after about 2300 UTC as the storm reached St. Louis.

Partly because of a forecast of potential severe weather near St. Louis made the previous evening, and weather resulting from the passage of the IOP-7 MCS through St. Louis early on the morning of 10 June, both P-3s were diverted to Des Moines, Iowa, after completing their portion of IOP 7. Because severe weather threatened the St. Louis area, the Learjet was deployed to Moline, Illinois. These decisions turned out to be fortuitous, because subsequent events created a severe hazard at MidAmerica St. Louis Airport for parked aircraft. The bow echo reached MidAmerica St. Louis Airport at 2315 UTC (Fig. 10). The Belleville control tower estimated wind gusts as high as 45 m s⁻¹. A Navy C-130 transport plane parked at MidAmerica suffered severe damage to its nose and landing gear. Power was immediately lost as power lines and even several miles of power poles in the area were blown down.

An extensive damage survey of this event is summarized in Fig. 11. Six tornado tracks were identified, as well as a swath of straight-line wind damage equivalent to F0 on the Fujita scale. This swath was about 10 km wide and 60 km long. As the bow echo approached Centralia, Illinois, about 130 km to the east, damage abruptly stopped despite the fact that the system essentially maintained its structure and forward speed.

(Fig. 4) that began moving rapidly eastward toward St. Louis. Hail as large as 4 cm in diameter was reported with the developing convective line. The line became oriented in a north–south direction and accelerated to a ground relative speed of about 35 m s⁻¹. According to a special 1800 UTC sounding from Springfield, Missouri (about 100 km south of the location where the first cells developed), the wind was westerly or southwesterly at all levels with a vertical wind shear of about 15 m s⁻¹ between the surface and 700 hPa and weak shear between 700 and 250 hPa. Data from the 404-MHz NOAA profiler at Conway, Missouri (about 50 km to the northeast of Spring-

With the loss of power at the BAMEX operations center, a new temporary center was established at a nearby hotel within an hour. Unfortunately, no BAMEX facilities were able to directly observe this event, mainly because of crew rest requirements and the remarkable speed with which the MCS moved to the edge of the BAMEX domain. However, sufficient operational data exist to address some questions regarding damaging winds and tornadoes.

Cloud microphysics measurements. During BAMEX, the NOAA P-3 executed 16 spiral descents within stratiform regions of MCSs, sometimes directly behind developing bows, other times farther to the rear of convective lines and at various stages in their evolution. Each descent was made between temperatures of approximately −10° and +10°C, so that hydrometeor populations above, within, and below the melting layer were sampled. During these Lagrangian spirals, the pilots allowed the aircraft to drift with the wind. Spirals typically took 15–30 min in an attempt to sample the same population of particles falling at roughly 1 m s$^{−1}$ above the melting layer and 5 m s$^{−1}$ below. In other cases, descent rates were larger above the melting layer to avoid lightning strikes (P-3 aircraft have a notorious tendency to electrically charge while flying in the mixed phase region from 0° to −5°C). The data are unique in that they are the first observations of the microphysical structure of the stratiform region behind bow echoes acquired in conjunction with high-quality Doppler observations.

Figure 12 shows particle images as a function of temperature derived during a spiral descent on 29 June 2003 (IOP 14). The observations shown were acquired with a 2D-C, which measures the sizes, shapes, and concentrations of particles with nominal sizes between 50 and 1600 μm; the P-3 was also equipped with a two-dimensional precipitation probe for detecting particles with sizes between 200 and 6400 μm. During the descent shown in Fig. 12, graupel (the rough, quasi-circular particle images) was found down to temperatures of +7°C before completely melting to raindrops (circular images). At the time these observations were acquired, the NOAA radar indicated a significant slope in the bright band with the melting layer extending to progressively lower heights toward the line. Particle images obtained during other spiral descents in other MCSs did not show graupel and frozen particulates extending to such low altitudes because the observations were acquired at different locations behind the convective line and at different stages in the system's life cycle. Current research is devoted to analyzing the varia-

0.5° Reflectivity and Velocity from LSX
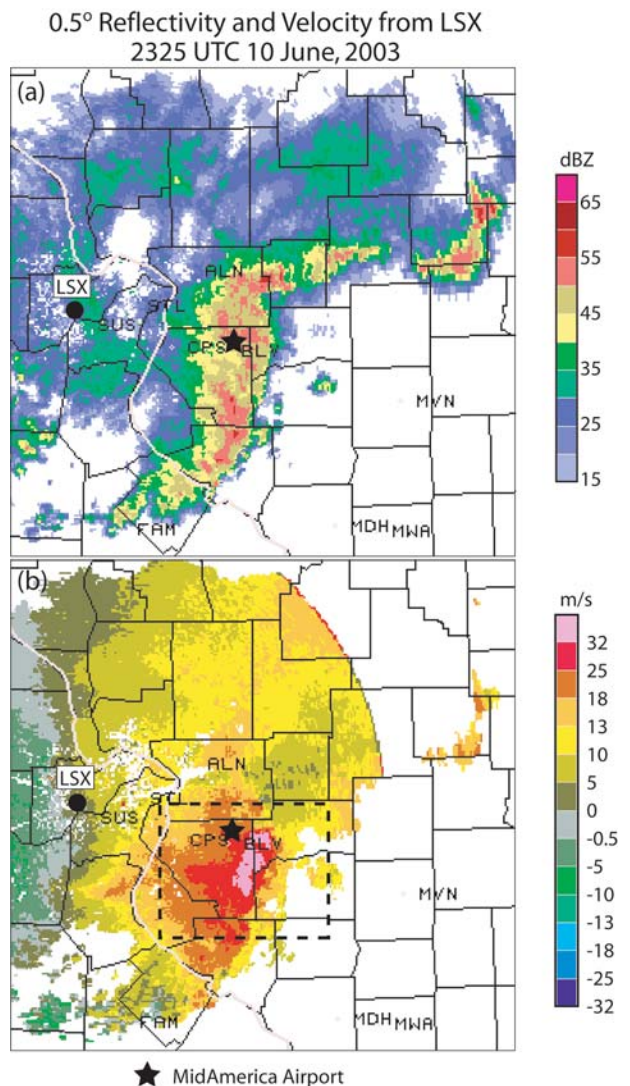2325 UTC 10 June, 2003

FIG. 10. (a) Reflectivity and (b) radial velocity from the St. Louis (LSX) WSR-88D lowest scan at 2325 UTC 10 Jun 2003. The black dot indicates the location of LSX, the black star is MAA. Domain shown is about 250 km on a side.

tions in the microphysical properties of the spirals in context of the meteorological situation and distance from the bow in order to understand and quantify the role of aggregation, melting, and evaporation in the melting layer on the evolution of bow echoes.

The MCV of IOP 1. As shown in Fig. 4, a bow echo preceded the MCV of IOP 1 (24–25 May). The bow echo formed over Nebraska during the evening of 24 May, moved south-southeastward, and merged with another convective line forming in Kansas. The bow echo moved into Oklahoma around 1200 UTC before dissipating southeast of Oklahoma City around 1700 UTC. This system produced a long-lived MCV
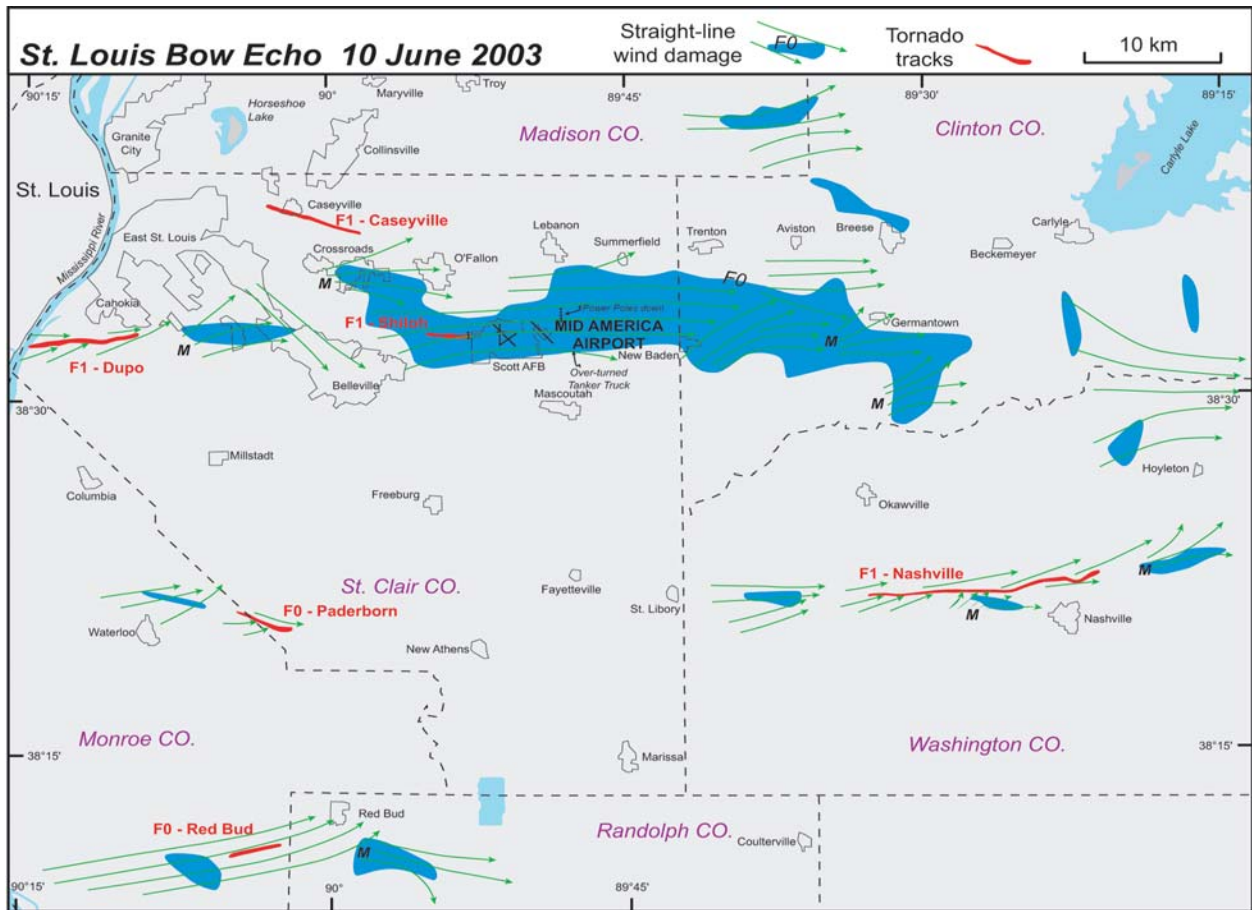
Fig. 11. Damage survey from 10 Jun 2003 severe bow echo near MidAmerica St. Louis Airport. Blue shading denotes straight-line winds with damage equivalent to F0. Green arrows indicate wind direction inferred from debris orientation. Individual tornado tracks are denoted by heavy red lines. Time of damage ranged from about 2300 UTC 10 Jun to 0000 UTC 11 Jun. Domain is box with dashed line in Fig. 10.

within which moderate and occasionally heavy stratiform rain with embedded deep convection was maintained throughout the day.

The MCV in IOP 1 was unique because it was sampled by all three aircraft. Only dropsondes from the WMI Learjet will be discussed here. Thirty-one dropsondes were released during two sampling periods—the first from 1614 to 1734 UTC, and the second from 1950 to 2234 UTC. The ground-relative locations of these dropsondes are shown in Fig. 13. Nearly all drops were made from 180–190 hPa. There were problems recording winds on some soundings, but good thermodynamic data were obtained from all soundings.

To enhance the dropsonde data in the analysis, we included profiler observations from times during the drop periods. Soundings and profilers were time–space-corrected relative to approximately the central time of each flight (1700 and 2100 UTC, respectively). The vortex motion, determined from animations of

radar and satellite data, was about 12 m s^{-1} from 280°. This motion changed little during the day. Thus, it was straightforward to merge the two time–space-corrected datasets. Those merged data at 600 hPa appear in Fig. 14, plotted in a vortex-relative spatial coordinate with the vortex motion subtracted. A composite dropsonde profile was used to convert height to pressure at profiler locations.

The plotted winds in Fig. 14 revealed a clear cyclone circulation centered over northwestern Arkansas with a radius of maximum wind near or slightly less than 100 km. The axis of the vortex appeared elongated from west-northwest to east-southeast, along the direction of both the vortex motion and the mean wind shear between 900 and 500 hPa, the latter being deduced from averaging the dropsondes. The maximum tangential wind was estimated between 12 and 15 m s^{-1}. There was little evidence of temperature perturbations in the core, suggesting that 600 hPa is close to the level of maximum
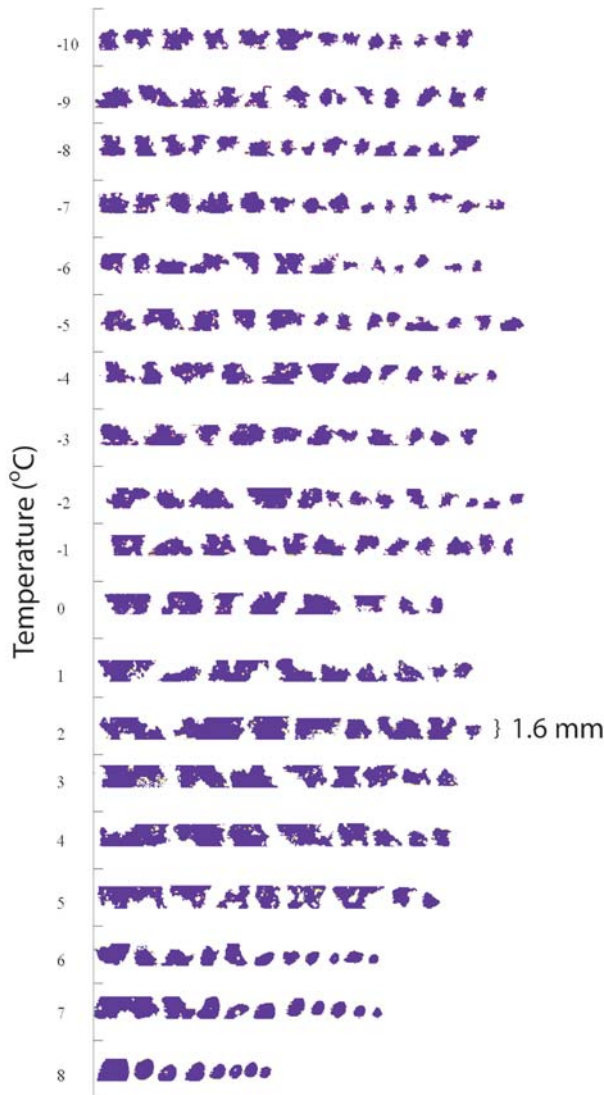
Fɪɢ. 12. Images from the 2D-C probe during an advecting spiral descent behind a bow echo on 29 Jun 2003 displayed as a function of temperature. Each row is 1.6 mm from top to bottom.

Fɪɢ. 13. Mesoscale convective vortex observed by visible satellite (*NOAA-14* polar orbiter) at 1950 UTC 24 May (IOP 1). Black and white arrows schematically depict vortex-relative winds. Blue arrow indicate system trajectory. Orange dots mark dropsonde locations. "X" marks the vortex center. Large vorticity extends westward along the thin solid line.
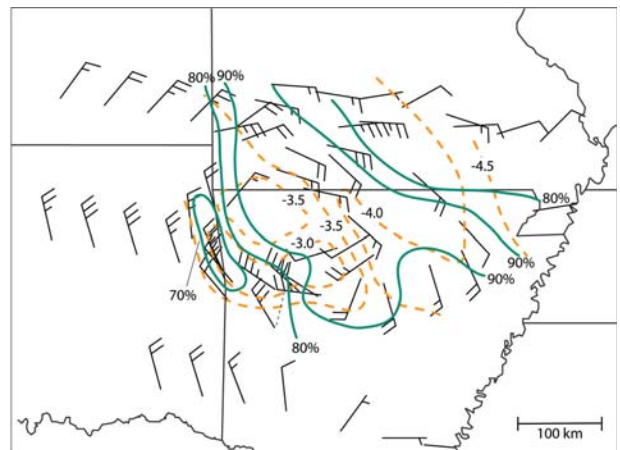
Fɪɢ. 14. Space–time-corrected analysis of dropsonde and wind profiler data at 600 hPa for the MCV of IOP 1. Winds are system relative; long barbs denote wind speed of 5 m s⁻¹; short barbs denote wind speed of 2.5 m s⁻¹. Temperature (orange) is analyzed in 0.5°C increments; relative humidity (green) is analyzed in increments of 10%. Effective valid time is 1900 UTC 24 May 2003.

tangential winds to the extent that hydrostatic and gradient balance is valid. The main thermal and kinematic feature was a wind shift to the southeast of the vortex center. Ahead of this wind shift was moist southeasterly flow (relative to the vortex) in which a band of moderate rain occurred (not shown). The southeasterly current turned to easterly as it passed to the north of the vortex where the most concentrated area of cloudiness was (Fig. 13). To the south of the vortex, the westerlies were slightly warmer and drier on this pressure level, but as one moved lower to the 900–800-hPa layer, the relative humidity decreased to below 60% (not shown). This lower-tropospheric dryness could be traced to subsidence
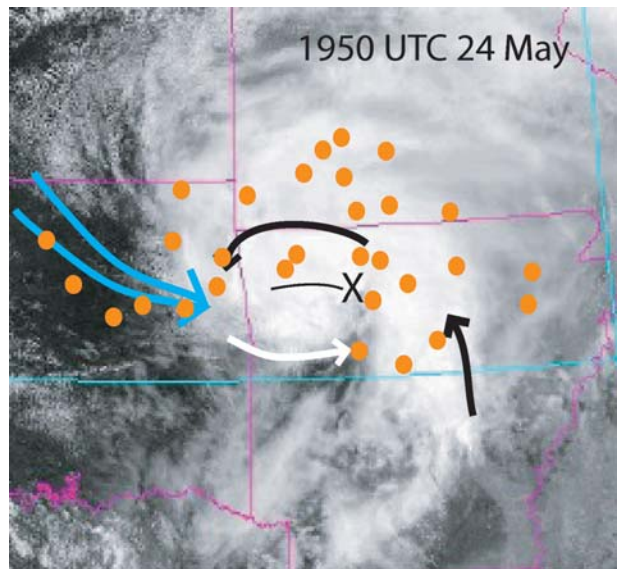
behind the bow echo over northern Oklahoma earlier in the day. At 600 hPa, the driest air sampled by the dropsondes was located in the southwest quadrant of the vortex, perhaps indicative of mesoscale subsidence induced by the MCV. Overall, these observations, combined with airborne dual-Doppler and

ground-based single Doppler radar, represent the best MCV dataset to date.

SUMMARY AND RESEARCH OPPORTUNITIES.

This article has summarized the scientific goals and observing facilities, and provided preliminary analyses of select cases from BAMEX. The project was designed to sample MCSs capable of producing damaging surface winds and capable of producing long-lived MCVs, as well as to observe MCVs in their mature state relatively devoid of convection. In the latter objective, we emphasized observations that would help illuminate how new convection is initiated near MCVs. The project may also be summarized as an exploration of MCSs that feature strong mesoscale rotation (about a vertical axis), often simultaneously on different spatial scales, and the mechanisms by which these rotational structures affect and are modified by convection.

During BAMEX, new procedures were implemented regarding the deployment of multiple observing facilities in and near MCSs. The system-following strategy and high mobility of the observing platforms (three aircraft and an array of ground-based systems) allowed us to cover a large domain, sampling MCSs in different geographical regions and in different environments. The complete summary of operations is available on the BAMEX Field Catalog (online at www.joss.ucar.edu/bamex/catalog/).

Several lessons in operations were learned. First, it is possible to conduct multiple aircraft operations in the vicinity of severe convective systems with proper nowcasting, flight direction, and coordination with air traffic authorities. Second, real-time flight-track information and reliable aircraft-to-aircraft and aircraft-to-ground communication is vital for making highly resolved measurements in the vicinity of developing or mature convective systems. Third, it is important to have nowcasting support in the operations center during developing convective situations so that direct communication is possible between aircraft coordinators, nowcasters, and airborne mission scientists. Satellite-based communications (voice, data, and text) maximized flexibility in operations and allowed us to achieve science objectives, while assuring safe operations in complex weather situations.

The emerging scientific opportunities from BAMEX and near-term research directions are diverse and many have fundamental implications for mesoscale studies. We observed a multitude of mesoscale vortices within MCSs covering a range of scales, sometimes even within the same system. The

basic mechanism of up-scale growth of vortical circulations is an open question, but can be addressed with the data collected. Second, regarding long-lived MCVs, we observed on more than one occasion that the vortex circulation was clearly visible at the surface. Furthermore, the MCV seemed to enhance the poleward transport of high equivalent potential temperature air in the lower troposphere, which dramatically altered the moist thermodynamic stability of the atmosphere locally.

Some important issues regarding the rear-inflow and mesoscale downdraft currents within MCSs have emerged. The rear inflow was observed to be remarkably deep in some systems, extending up to at least 7 km, while in others it did not extend much above 4 km. What governs this variation? In addition, the greatest damage was typically not observed to occur in the most pronounced, extensive bow echoes, but rather in smaller bows perhaps 100 km in length or less. Why?

Data from BAMEX will also provide valuable information for the verification of mesoscale and cloud-system resolving models such as WRF, MM5, and RAMS. In particular, verification of hydrometeor concentration, mesoscale kinematic structure, and thermodynamic profiles within and in the environment of convective systems are possible to a much greater extent than before BAMEX. Furthermore, the relatively fine spacing of sounding data and their systematic deployment near convective systems will allow greater examination of mesoscale predictability and the effect of targeted observations on predictive skill. It will also allow development and testing of advanced data assimilation techniques (F. Zhang 2003, personal communication). Finally, the data exist to also test numerous hypotheses about observable precursors of severe surface winds.

In conclusion, the 18 IOPs and other special observations constitute an unprecedented dataset for the study of the life cycle of mesoscale convective systems. While we have emphasized bow echoes and convective systems producing MCVs, there were several other cases that do not fit neatly into these two categories. These may provide null cases or force us to develop broader conceptualizations of MCS dynamics. Future papers by many of the authors of the present article and other researchers will report on case studies, composite analyses, and numerical simulations of BAMEX MCSs.

list everyone involved. Foremost, we are grateful to the National Science Foundation for funding the majority of the project. We are also grateful to NOAA's Aircraft Operations Center and the Naval Research Laboratory for their operation of the P-3s, especially their project managers, Jim McFadden (NOAA) and Brigitte Baeuerle (NCAR/ATD for the NRL P-3). In addition, we wish to thank the JOSS for their creation and maintenance of the BAMEX Field Catalogue and their oversight of operations.

Numerous forecasters were involved. From the NWS we wish to thank Llyle Barker (WFO ILX), Bill Nichols (WFO DVN), Dan Baumgardt (WFO ARX), Evan Bookbinder (WFO SGF), Christopher Buonanno (WFO LIT), Mark Britt (WFO LSX), Dan Spaeth (WFO PAH), Wes Browning (WFO SGF), Dan Smith (WFO ILX), Fred Glass (WFO LSX), Greg Koch (WFO EAX), Jason Puma (WFO IND), Mark Ratzer (WFO LOT), and Gary Schmocker (WFO LSX). We would also like to thank Eyad Atallah, Tom Galarneau, and Brandon Smith from The University at Albany, State University of New York for their forecasting assistance.

Dave Ahijevych from NCAR, Richard James from the Pennsylvania State University, Dan Hawblitzel from Texas A&M, and Sue van den Heever from Colorado State University performed valuable roles as dropsonde aircraft coordinators. We are grateful to many staff from the Atmospheric Technology Division of NCAR who were responsible for MGLASS, dropsonde, and ELDORA operations. Through the coordination of Dr. Ali Tokay, the National Aeronautics and Space Administration loaned a disdrometer for raindrop measurements at the MIPS site.

The authors would also like to acknowledge Hanne Murphey of UCLA for contributing Fig. 7 and the related analysis, and Kris Conrad of NCAR for drafting Fig. 2.

APPENDIX: DATA ACCESS AND ARCHIVES.

BAMEX participants worked from early in the planning phase to develop and implement a comprehensive data management strategy. JOSS, in close collaboration with the project scientists, has developed a data archive for all BAMEX research and operational datasets. Collection of operational data from the National Weather Service [NWS, WSR-88D level II data from 58 radars, 280 Automated Surface Observing System (ASOS) stations, etc.], special GPS precipitable water, and regional mesonetwork (24 states) sources were all obtained during the field phase. Data policy, data access, and format and documentation guidelines were all put in place with emphasis on the need to share a variety of data quickly and easily. Special data composites for surface and upper-air data will be prepared to save work on the part of each investigator to individually reprocess, quality control,

and reformat separate network datasets. Further details about BAMEX data management and access to all project datasets may be found online (www.joss.ucar.edu/BAMEX/dm/).

REFERENCES

Bartels, D. L., and R. A. Maddox, 1991: Midlevel cyclonic vortices generated by mesoscale convective systems. *Mon. Wea. Rev.,* **119**, 104–118.

——, J. M. Brown, and E. I. Tollerud, 1997: Structure of a midtropospheric vortex induced by a mesoscale convective system. *Mon. Wea. Rev.,* **125**, 193–211.

Bernardet, L. R., and W. R. Cotton, 1998: Multiscale evolution of a derecho-producing mesoscale convective system. *Mon. Wea. Rev.,* **126**, 2991–3015.

Bister, M., and K. Emanuel, 1997: The genesis of Hurricane Guillermo: TEXMEX analysis and a modeling study. *Mon. Wea. Rev.,* **125**, 2662–2682.

Blanchard, D. O., 1990: Mesoscale convective patterns of the Southern High Plains. *Bull. Amer. Meteor. Soc.,* **71**, 994–1005.

Bosart, L. F., and F. Sanders, 1981: The Johnstown flood of July 1977: A long-lived convective system. *J. Atmos. Sci.,* **38**, 1616–1642.

Brandes, E. A., 1990: Evolution and structure of the 6–7 May 1985 mesoscale convective system and associated vortex. *Mon. Wea. Rev.,* **118**, 109–127.

Burgess, D. W., and B. F. Smull, 1993: Doppler radar observations of a bow echo associated with a long-track severe windstorm. Preprints, *16th Conf. on Severe Local Storms,* Kananaskis Park, AB, Canada, Amer. Meteor. Soc., 203–208.

Coniglio, M. C., and D. J. Stensrud, 2001: Simulation of a progressive derecho using composite initial conditions. *Mon. Wea. Rev.,* **129**, 1593–1616.

Cotton, W. R., M.-S. Lin, R. L. McAnelly, and C. J. Tremback, 1989: A composite model of mesoscale convective complexes. *Mon. Wea. Rev.,* **117**, 765–783.

Cram, T. A., M. T. Montgomery, and R. F. A. Hertenstein, 2002: Early evolution of vertical vorticity in a numerically simulated idealized convective line. *J. Atmos. Sci.*, **59**, 2113–2127.

Cunning, J. B., 1986: The Oklahoma–Kansas Preliminary Regional Experiment for STORM-Central. *Bull. Amer. Meteor. Soc.*, **67**, 1478–1486.

Davis, C. A., and M. L. Weisman, 1994: Balanced dynamics of mesoscale vortices produced in simulated convective systems. *J. Atmos. Sci.,* **51**, 2005–2030.

——, and S. B. Trier, 2002: Cloud-resolving simulations of mesoscale vortex intensification and its effect on a serial mesoscale convective system. *Mon. Wea. Rev.,* **130,** 2839–2858.

——, D. A. Ahijevych, and S. B. Trier, 2002: Detection and prediction of warm season, midtropospheric vortices by the rapid update cycle. *Mon. Wea. Rev.,* **130**, 24–42.

Done, J., C. Davis, and M. Weisman, 2004: The next qeneration of NWP: Explicit forecasts of convection using the Weather Research and Forecasting (WRF) Model. *Atmos. Sci. Lett.,* submitted.

Evans, J. S., and C. A. Doswell III, 2001: Examination of derecho environments using proximity soundings. *Wea. Forecasting,* **16**, 329–242.

Fritsch, J. M., J. D. Murphy, and J. S. Kain, 1994: Warm core vortex amplification over land. *J. Atmos. Sci.,* **51**, 1780–1807.

Forbes, G. S., and R. M. Wakimoto, 1983: A concentrated outbreak of tornadoes, downbursts and microbursts, and implications regarding vortex classification. *Mon. Wea. Rev.,* **111**, 220–235.

Fujita, T. T., 1978: Manual of downburst identification for project NIMROD. Department of Geophysical Sciences, University of Chicago, Satellite and Mesometeorology Research Paper No. 156, 104 pp.

Funk, T. W., K. E. Darmofal, J. D. Kirkpatrick, V. L. Dewald, R. W. Przybylinski, G. K. Schmocker, and Y.-J. Lin, 1999: Storm reflectivity and mesocyclone evolution associated with the 15 April 1994 squall line over Kentucky and Southern Indiana. *Wea. Forecasting,* **14**, 976–993.

Grell, G. A., J. Dudhia, and D. R. Stauffer, 1994: A description of the fifth generation Penn State/NCAR mesoscale model. NCAR Tech. Note 398+STR A, 121 pp. [Available from National Center for Atmospheric Research, P.O. Box 3000, Boulder, CO 80303.]

Harr, P. A., and R. L. Elsberry, 1996: Structure of a mesoscale convective system embedded within Typhoon Robyn during TCM-93. *Mon. Wea. Rev.,* **124**, 634–652.

Houze, R. A., Jr., S. A. Rutledge, M. I. Biggerstaff, and B. F. Smull, 1989: Interpretation of Doppler weather radar displays of midlatitude mesoscale convective systems. *Bull. Amer. Meteor. Soc.,* **70**, 608–619.

——, B. F. Smull, and P. Dodge, 1990: Mesoscale organization of springtime rainstorms in Oklahoma. *Mon. Wea. Rev.,* **118**, 613–654.

Johns, R. H., and W. D. Hirt, 1987: Derechos: Widespread convectively induced windstorms. *Wea. Forecasting,* **2**, 32–49.

Jorgensen, D. P., and B. F. Smull, 1993: Mesovortex circulations seen by airborne Doppler radar within a bow-echo mesoscale convective system. *Bull. Amer. Meteor. Soc.,* **74**, 2146–2157.

——, T. Matejka, and J. D. DuGranrut, 1996: Multi-beam techniques for deriving wind fields from airborne Doppler radars. *J. Meteor. Atmos. Phys.,* **59**, 83–104.

——, T. R. Shepherd, and A. Goldstein, 2000: A multiple pulse repetition frequency scheme for extending the unambiguous Doppler velocity of the NOAA P-3 airborne Doppler radar. *J. Atmos. Oceanic Technol.,* **17**, 585–594.

Knievel, J. C., and R. H. Johnson, 2003: A scale-discriminating vorticity budget for a mesoscale vortex in a midlatitude, continental mesoscale convective system. *J. Atmos. Sci.,* **60**, 781–794.

Klimowski, B. A., R. Pyzybylinski, G. Schmocker, and M. R. Hjelmfelt, 2000: Observations of the formation and early evolution of bow echoes. Preprints, *20th Conf. on Severe Local Storms,* Orlando, FL, Amer. Meteor. Soc., 44–47.

Loehrer, S. M., and R. H. Johnson, 1995: Surface pressure and precipitation life cycle characteristics of PRE-STORM mesoscale convective systems. *Mon. Wea. Rev.,* **123**, 600–621.

Maddox, R. A., 1983: Large-scale meteorological conditions associated with midlatitude, mesoscale convective complexes. *Mon. Wea. Rev.,* **111**, 1475–1493.

Menard, R. D., and J. M. Fritsch, 1989: A mesoscale convective complex-generated inertially stable warm core vortex. *Mon. Wea. Rev.,* **117**, 1237–1260.

Michalakes, J., S. Chen, J. Dudhia, L. Hart, J. Klemp, J. Middlecoff, and W. Skamarock, 2001: *Developments in Teracomputing: Proceedings of the Ninth ECMWF Workshop on the Use of High Performance Computing in Meteorology.* W. Zwieflhofer and N. Kreitz, Eds., World Scientific, 269–276.

Miller, D. J., and R. H. Johns, 2000: A detailed look at extreme wind damage in derecho events. Preprints, *20th Conf. on Severe Local Storms,* Orlando, FL, Amer. Meteor. Soc., 52–55.

Montgomery, M. T., and J. Enagonio, 1998: Tropical cyclogenesis via convectively forced Rossby waves in a three-dimensional quasi-geostrophic model. *J. Atmos. Sci.,* **55**, 3176–3207.

Newton, C. W., 1950: Structure and mechanism of the pre-frontal squall line. *J. Meteor.,* **7**, 210–222.

Olsson, P. Q., and W. R. Cotton, 1997: Balanced and unbalanced circulations in a primitive equation simulation of a midlatitude MCC. Part II: Analysis of balance. *J. Atmos. Sci.,* **54**, 479–497.

Pfost, R. L., and A. E. Gerard, 1997: "Bookend vortex" induced tornadoes along the Natchez Trace. *Wea. Forecasting,* **12**, 572–580.

Pielke, R. A., and Coauthors, 1992: A comprehensive meteorological modeling system—RAMS. *Meteor. Atmos. Phys.,* **49**, 69–91.

Przybylinski, R. W., 1995: The bow echo: Observations, numerical simulations, and severe weather detection methods. *Wea. Forecasting.,* **10**, 203–218.

——, G. K. Schmocker, and Y.-J. Lin, 2000: A study of storm and vortex morphology during the "intensifying stage" of severe wind mesoscale convective systems. Preprints, *20th Conf. on Severe Local Storms,* Orlando, FL, Amer. Meteor. Soc., 173–176.

Raymond, D. J., and H. Jiang, 1990: A theory for long-lived mesoscale convective systems. *J. Atmos. Sci.,* **47**, 3067–3077.

——, C. López-Carillo, and L. López Cavazos, 1998: Case studies of developing east Pacific easterly waves. *Quart. J. Roy. Meteor. Soc.,* **124**, 2005–2034.

Rogers, R. F., and J. M. Fritsch, 2001: Surface cyclogenesis from convectively driven amplification of midlevel mesoscale convective vortices. *Mon. Wea. Rev.,* **129**, 605–637.

Ritchie, E. A., and G. Holland, 1997: Scale interaction during the formation of Typhoon Irving. *Mon. Wea. Rev.,* **125**, 1377–1396.

Schmocker, G. K., R. W. Przybylinski, and Y.-J. Lin, 1996: Forecasting the initial onset of damaging downburst winds associated with a mesoscale convective system (MCS) using the mid-altitude radial convergence (MARC) signature. Preprints, *15th Conf. on Weather Analysis and Forecasting,* Norfolk, VA, Amer. Meteor. Soc., 306–3ll.

——, ——, and E. N. Rasmussen, 2000: The severe bow echo event of 14 June 1998 over the mid-Mississippi valley region: A case of vortex development near the intersection of a preexisting boundary and a convective line. Preprints, *20th Conf. on Severe Local Storms,* Orlando, FL, Amer. Meteor. Soc., 169–172.

Scott, J. D., and S. A. Rutledge, 1995: Doppler radar observations of an asymmetric mesoscale convective system and associated vortex couplet. *Mon. Wea. Rev.,* **123**, 3437–3457.

Skamarock, W. C., M. L. Weisman, and J. B. Klemp, 1994: Three-dimensional evolution of simulated long-lived squall lines. *J. Atmos. Sci.,* **51**, 2563–2584.

Smull, B. F., and R. A. Houze Jr., 1987: Rear inflow in squall lines with trailing stratiform precipitation. *Mon. Wea. Rev.,* **115**, 2869–2889.

Trapp, R. J., and M. L. Weisman, 2003: Low-level mesovortices within squall lines and bow echoes. Part II: Their genesis and implications. *Mon. Wea. Rev.,* **131**, 2804–2823.

——, E. D. Mitchell, G. A. Tipton, D. W. Effertz, A. I. Watson, D. L. Andra Jr., and M. A. Magsig, 1999: Descending and non-descending tornadic vortex signatures detected by WSR-88Ds. *Wea. Forecasting,* **14**, 625–639.

——, S. A. Tessendorf, E. S. Godfrey, and H. E. Brooks, 2004: Tornadoes from squall lines and bow echoes. Part I: Climatological distribution. *Wea. Forecasting,* submitted.

Trier, S. B., and C. A. Davis, 2002: Influence of balanced motions on heavy precipitation within a long-lived convectively generated vortex. *Mon. Wea. Rev.,* **130**, 877–899.

——, ——, and J. D. Tuttle, 2000: Long-lived mesoconvective vortices and their environment. Part I: Observations from the central United States during the 1998 warm season. *Mon. Wea. Rev.,* **128**, 3376–3395.

Weisman, M. L., 1993: The genesis of severe, long-lived bow echoes. *J. Atmos. Sci.,* **50**, 645–670.

——, 2001: Bow echoes: A tribute to T. T. Fujita. *Bull. Amer. Meteor. Soc.,* **82**, 97–116.

——, and C. Davis, 1998: Mechanisms for the generation of mesoscale vortices within quasi-linear convective systems. *J. Atmos. Sci.,* **55**, 2603–2622.

——, and R. J. Trapp, 2003: Low-level mesovortices within squall lines and bow echoes. Part I: Overview and dependence on environmental sheer. *Mon. Wea. Rev.,* **131**, 2779–2803.